



EXTRACTION OF SPATIO-TEMPORAL SLIP VELOCITY FUNCTION OF EARTHQUAKE FROM THE EXISTING SOURCE INVERSION MODEL

Hiroshi TAKENAKA¹, Yushiro FUJII², Ken MIYAKOSHI³,
Hiroshi KAWASE⁴ and Tomotaka IAWATA⁵

SUMMARY

The slip velocity function is one of the key factors controlling the radiation of seismic waves. We propose a technique for extracting a spatio-temporal slip velocity function from source time functions obtained by the existing conventional source inversion results. We also demonstrate the feasibility of this method with application to the inverted source models of the 26-March-1997 Northwestern Kagoshima earthquake (M_w 6.1) in Japan from teleseismic data and strong-motion data, respectively. The slip velocity function extracted from the strong-motion inversion model has a higher resolution both in space and time compared to that from the teleseismic inversion model. The maximum peak velocity in the asperity area for both models are comparable to those for the 1995 Kobe earthquake estimated by previous studies.

INTRODUCTION

Estimation of slip velocity function over the source fault of target earthquake is important to accomplish precise strong ground motion prediction. Because the slip velocity function is one of the key factors controlling the radiation of seismic waves. In particular, the larger slip velocity, which are mainly occurred on the asperity area of the fault plane, has a significant effect on the strong ground motion in broad area. Also even relatively small slip velocity could affect near-source ground motions. Although recently slip-velocity estimation technique are developed by forward modelling (e.g. Matsushima and Kawase [1]), and inversion method (e.g. Sekiguchi *et al.* [2]) using dense near-source records, most of events are analysed to obtain spatio-time moment rate functions by the conventional kinematic source inversion methods. Kinematic source inversion techniques such as the multi-time window linear inversion have been widely applied to broadband seismic records including teleseismic and strong-ground motion records to estimate

¹ Faculty of Sciences, Kyushu University, Japan. Email: takenaka@geo.kyushu-u.ac.jp

² Graduate School of Science, Kyushu University, Japan. Email: fujii@geo.kyushu-u.ac.jp

³ Geo-Research Institute, Japan. Email: ken@geor.or.jp

⁴ Faculty of Human-Environmental Studies, Kyushu University, Japan.
Email: kawase@seis.arch.kyushu-u.ac.jp

⁵ Disaster Prevention Research Institute, Kyoto University, Japan.
Email: iwata@egmdpri01.dpri.kyoto-u.ac.jp

spatio-temporal slip distributions on fault planes of middle to large earthquakes since Olson and Apsel [3] or Hartzell and Heaton [4]. In kinematic source inversion source fault is conventionally divided into many subfaults to express spatial variation, and each subfault is represented by a single or multiple point sources placed at constant intervals on the planar surface. Such conventional subfault discretization is convenient for the representation of spatial distribution of slip in kinematic source inversion. However, it is not continuous at the subfault boundaries, and the inversion results (source time function of each point source such as the moment release time history) include not only a slip time function but also a rupture propagation effect inside each subfault. Therefore such inversion results may not be directly suitable for physically meaningful investigation on slip velocity itself, and may not be directly available for fine-scale numerical modeling such as the FDM computation, of which grid spacing is much smaller than the subfault size, to simulate near-fault strong-ground motion or to calculate stress field on the fault planes for dynamic source analysis.

In this study we propose a method for extracting a spatio-temporal slip velocity function from source time functions obtained by the conventional source inversion. The derived slip velocity function is continuous everywhere in space and time. We demonstrate the feasibility of this method with application to the inverted source models of the 26-March-1997 Northwestern Kagoshima earthquake ($M_w 6.1$) in Japan.

METHOD

The spatio-temporal distribution of slip velocity is expanded with the linear b-spline basis functions in 2D space and time (Figure 1). Each linear b-spline function is an isosceles triangle defined by three knots, and thus this discretization can give a slip distribution continuous everywhere spatially and temporally. This approach is similar to that employed by Ide and Takeo [5] and Wu *et al.* [6] for a kinematic source inversion, but slightly different from theirs. In our approach the representation of slip velocity has an explicit rupture propagation term so that the effect of the rupture propagation under "the sub-grid level" (sub-subfault level) is involved in the slip velocity at any position over the fault plane. In our representation unlike theirs, it is possible to treat even rupture velocity variation of sub-subfault level if we have its information. The expansion coefficients are determined by fitting the spatial integration of slip velocity over each subfault in a least squares sense with some constraints to the contribution of the subfault derived from the conventional kinematic source inversion.

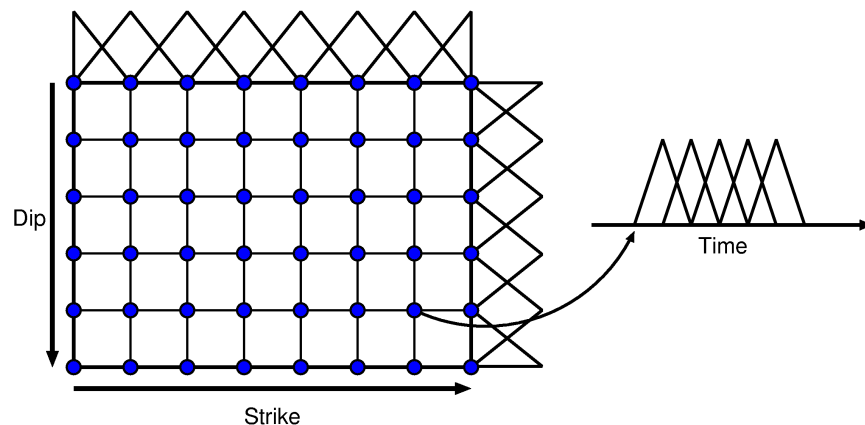


Figure 1. Configuration of the b-spline functions for the spatio-temporal representation of slip velocity and their knots on the fault plane. The knots of the spatial b-spline functions are located at the vertices of the subfaults.

APPLICATION TO THE 26-MARCH-1997 NORTHWESTERN KAGOSHIMA EARTHQUAKE

We apply our technique to the 26-March-1997 Northwestern Kagoshima, Japan, earthquake ($M_{JMA}6.5$) to demonstrate the feasibility of this method. Two moderate earthquakes ($M_{JMA}6.5$, $M_{JMA}6.3$) occurred in northwestern region of Kagoshima prefecture, Japan on March 26, 1997 and May 13, 1997 (JST; JST = UT + 9 hours). Locations of the two main events and those aftershocks occurring from 26 March 1997 to 17 September 1998, which are determined by the SEVO, Kyushu Univ., are shown in Figure 2 with the focal mechanisms estimated by the Japan Meteorological Agency (JMA). The 1997 Northwestern Kagoshima earthquakes are one of rare cases among inland large earthquakes, that the second main event occurred about one month and a half later after the first main event. The second main event has almost the same magnitude as that of the first one and is estimated to be a multiple shock consisting of a E-W fault and the N-S conjugate fault (see Figure 2).

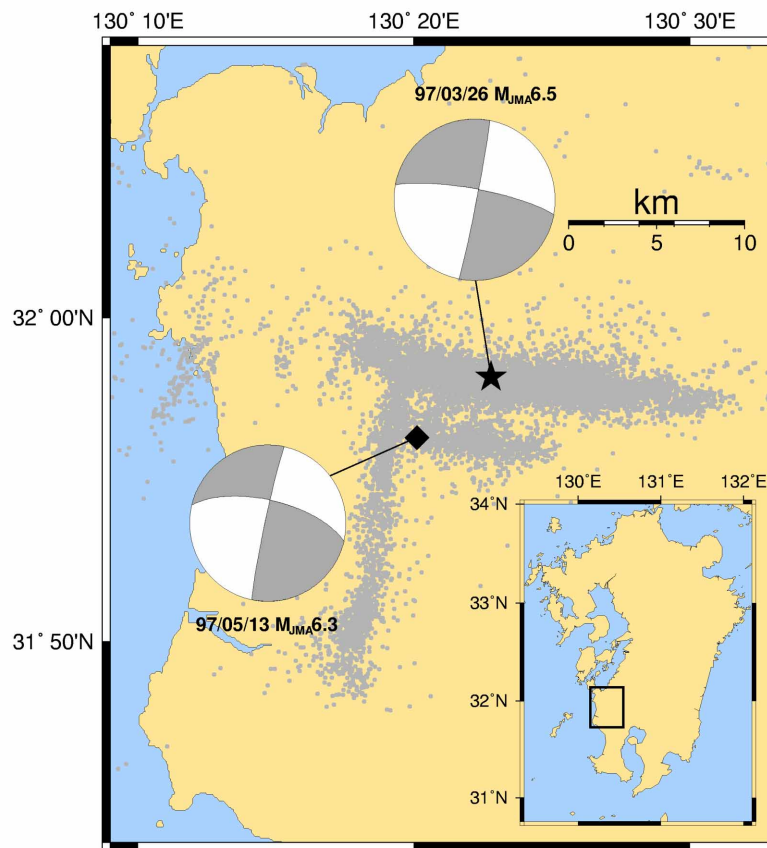


Figure 2. Map of the 1997 Northwestern Kagoshima earthquakes ($M_{JMA}6.5$ and $M_{JMA}6.3$). The focal mechanisms and aftershock distribution are shown, which were determined by the Japan Meteorological Agency and the SEVO, Kyushu Univ., respectively.

In this paper we choose two inverted source models of the first main event for extracting the slip velocity functions from them by our method: one is derived from teleseismic body wave data (Fujii *et al.* [7]), and the other is near-field strong-motion data (Miyakoshi *et al.* [8]).

Source Model from Teleseismic Body Waves

Fujii *et al.* [7] have inferred the source processes from teleseismic body waves (Figure 3). The fault plane was assumed to be a vertical plane of 21 km along the strike by 15 km downdip, with a strike of $N280^\circ E$, where the hypocentre ($31.96959^\circ N$, $130.37997^\circ E$, 8.213 km deep by the SEVO) locates just at the central position of the fault plane (Figure 3(a)). The fault plane was divided into 35 subfaults of 3 km-by-3 km, where each subfault is represented by 9 point sources placed at regular intervals on the surface. In their inversion, the focal mechanism was assumed to be pure strike-slip, and the slip vector then consists of two components with rakes of -45° and 45° . The source time function for each rake direction at each point source, which is identical over each subfault, is represented as a piece-wise linear function with line segment of 0.4 s time interval by using three to five b-spline functions with base of 0.8 s (i.e., multi-time windows), so that the unknown parameters of this inversion are the height of the b-spline functions. The rupture velocity for specifying the onset time of source time function at each point source in the inversion was assumed to be 2.5 km/s.

The result of this inversion is shown in Figures 3(b) and (c). Figure 3(b) indicates total slip over each subfault, and Figure 3(c) displays the derived source time functions of each subfault that has a physical dimension of the slip velocity. Since the dip component was so small as to be negligible, the strike components are only shown in Figures 3(b) and (c). We will also use only the strike component of the source time function to extract the slip velocity functions later.

Source Model from Strong-Motion Data

Another model for application of our method has been a model prepared by Miyakoshi *et al.* [8], which was derived from strong-motion records, and has a spatio-temporally more high-resolution compared to that of the teleseismic inversion shown above. In order to obtain the high-resolution source model reliable in the frequency range up to 2 Hz, they estimated the 1D underground structure model just under each strong-motion station (K-NET) from aftershock records by a R/V (Radial/Vertical) receiver function method, and then used it for the Green function calculations. The multi-time window linear inversion technique they used is similar to that used in the teleseismic inversion mentioned above. The geometry of the fault plane, a vertical plane, is shown in Figure 4(a), where the hypocentre locates at $31.978^\circ N$, $130.360^\circ E$, 7.6 km deep that was determined by the JMA. It is a little different from that employed in the teleseismic inversion. The geometrical relation between the fault plane used in teleseismic and strong-motion inversions is shown in Figure 5.

In the strong-motion inversion the size of subfaults was three times smaller than those of the teleseismic inversion, and each subfault has a single point source placed at the centre. The moment rate functions for two slip components at each point source, which are represented to be a piece-wise exponential function with line segment of 0.15 s time interval by using seven element functions with support of 0.3 s (i.e., multi-time windows) that are the first derivative of the smoothed ramp with rise time of 0.3 s, so that the unknown parameters of this inversion are the height of the element functions.

We show the result of their inversion in the case of the rupture velocity of 2.5 km/s in Figures 4(b) and (c). Figure 4(b) indicates total slip over each subfault, and Figure 4(c) displays the source time functions of each subfault that has been converted from the derived moment time function into a quantity with physical dimension of the slip velocity. In this inversion the dip component was also so small as to be negligible, the strike components are only shown in Figures 4(b) and (c). We will also use only the strike component of the source time function to extract the slip velocity functions later.

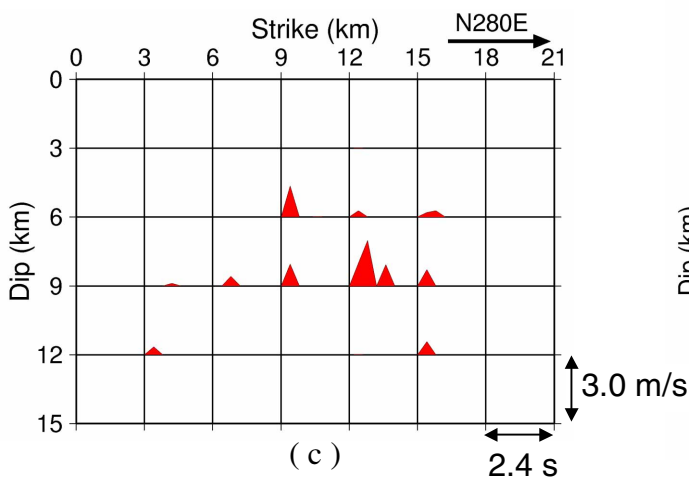
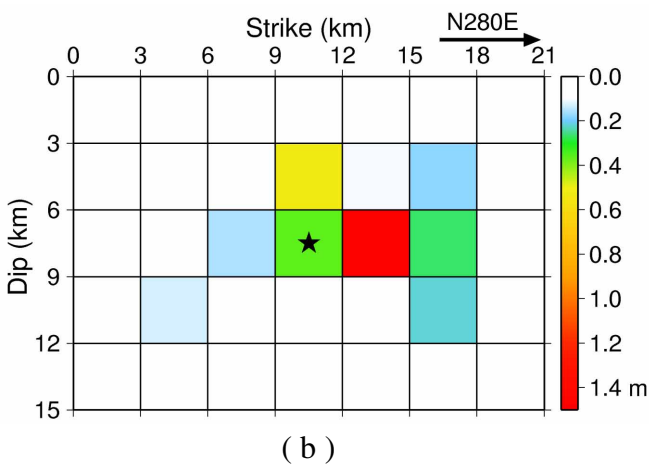
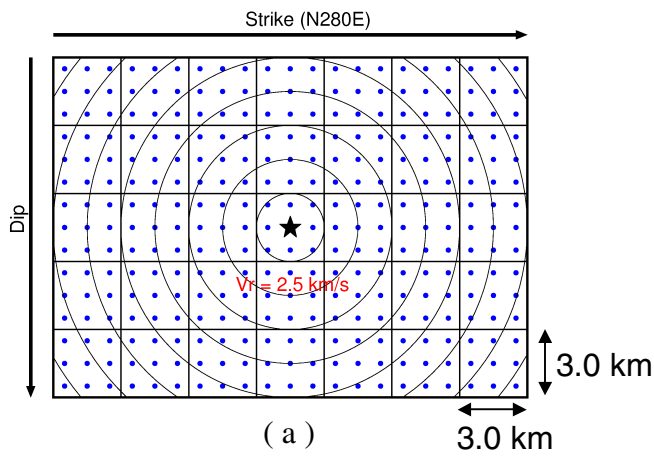


Figure 3. Source inversion of the Kagoshima earthquake ($M_{JMA}6.5$) from the teleseismic data. Top: fault discretization. Middle: slip in the strike direction. Bottom: source time function of the point sources on each subfault..

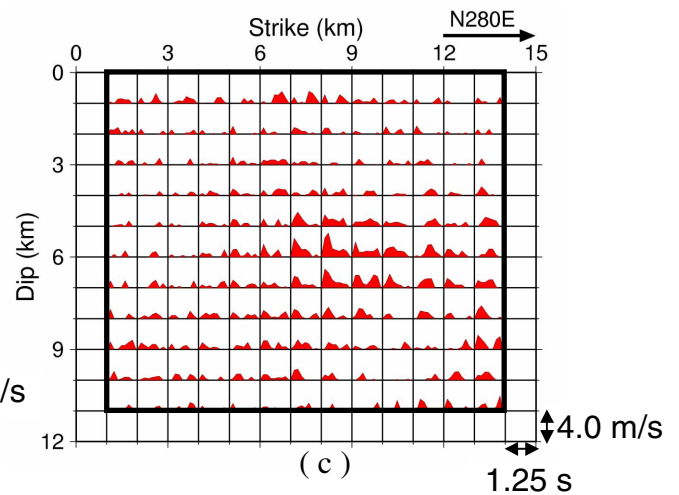
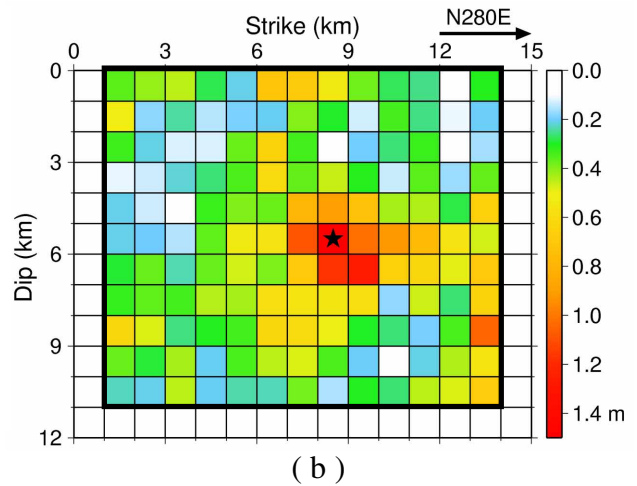
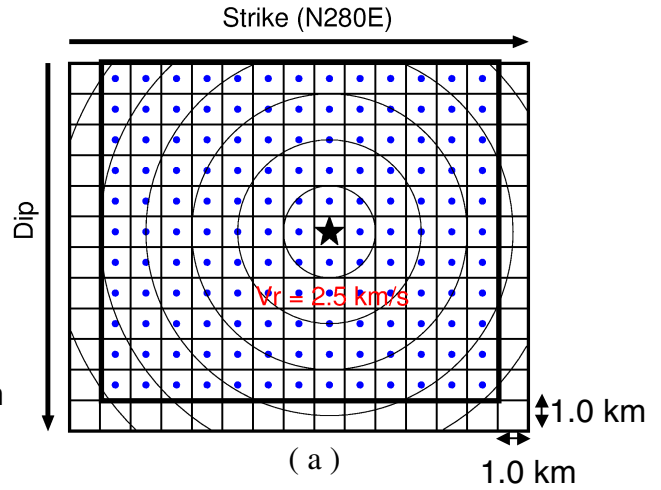


Figure 4. Source inversion of the Kagoshima earthquake ($M_{JMA}6.5$) from the strong-motion data. Top: fault discretisation. Middle: slip in the strike direction. Bottom: source time function of the point sources on each subfault.

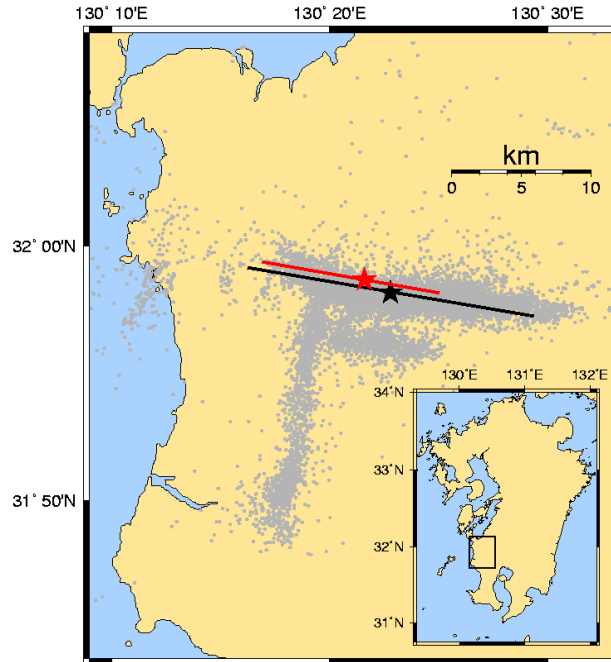


Figure 5. Locations of the fault plane models used for the teleseismic source inversion (black line) and the strong-motion inversion (red line). Star mark on each fault line indicates the epicentre location employed for each inversion.

Extraction of Slip Velocity Function

We now apply the present method to both source models from the teleseismic and the strong-motion inversions. In the application to the teleseismic inversion result, we use the b-spline functions with support of 6 km and 0.4 s for space and time discretisation, respectively, while in the application to the strong-motion inversion we employ the b-spline functions with support of 2 km and 0.2 s for space and time discretisation, respectively. The knots of the spatial b-spline functions are located at the vertices of the subfaults (see Figure 1). The number of time b-spline functions are eight and 11 for application to the teleseismic and the strong-motion inversions, respectively.

We show the results of application for the teleseismic inversion in Figures 6 and 8, and those for the strong-motion in Figures 7 and 9. Figures 6 and 7 display the slip velocity functions at the spatial knots (vertices of the subfaults), which are direct solution of our method. From them slip velocity functions and slip at any positions of the fault planes can be calculated. Figures 8 and 9 show total slip distribution over the fault planes and slip velocity functions at representative positions on the fault planes. From these figures it is found that in the both cases the derived slip velocity functions have a Kostrov-type feature (Kostrov [9]), i.e. a steep rise and gentle decay, and have higher peak values in the asperity area compared to in the non-asperity area. The maximum peak velocity is 3 km/s for the teleseismic inversion case, while for the strong-motion inversion case it is 6 km/s. The difference in the maximum peak velocity between both cases is ascribed to the difference the spatial and temporal resolution between them. Taking into account the resolution difference between the teleseismic and the strong-motion inversions, the slip velocity functions extracted in both cases are consistent each other.

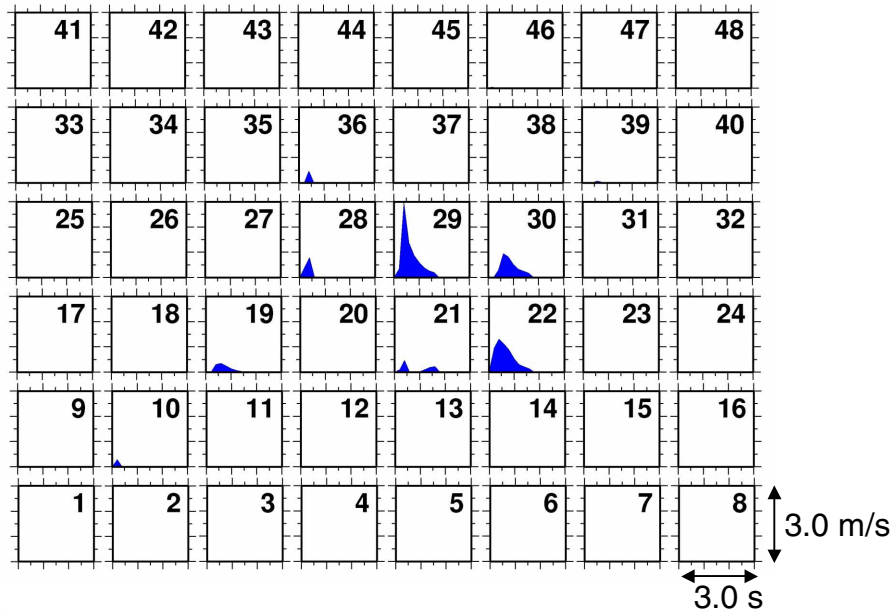


Figure 6. Slip velocity functions at the knots (vertices of subfaults) on the fault plane, extracted from the telesismic inversion model.

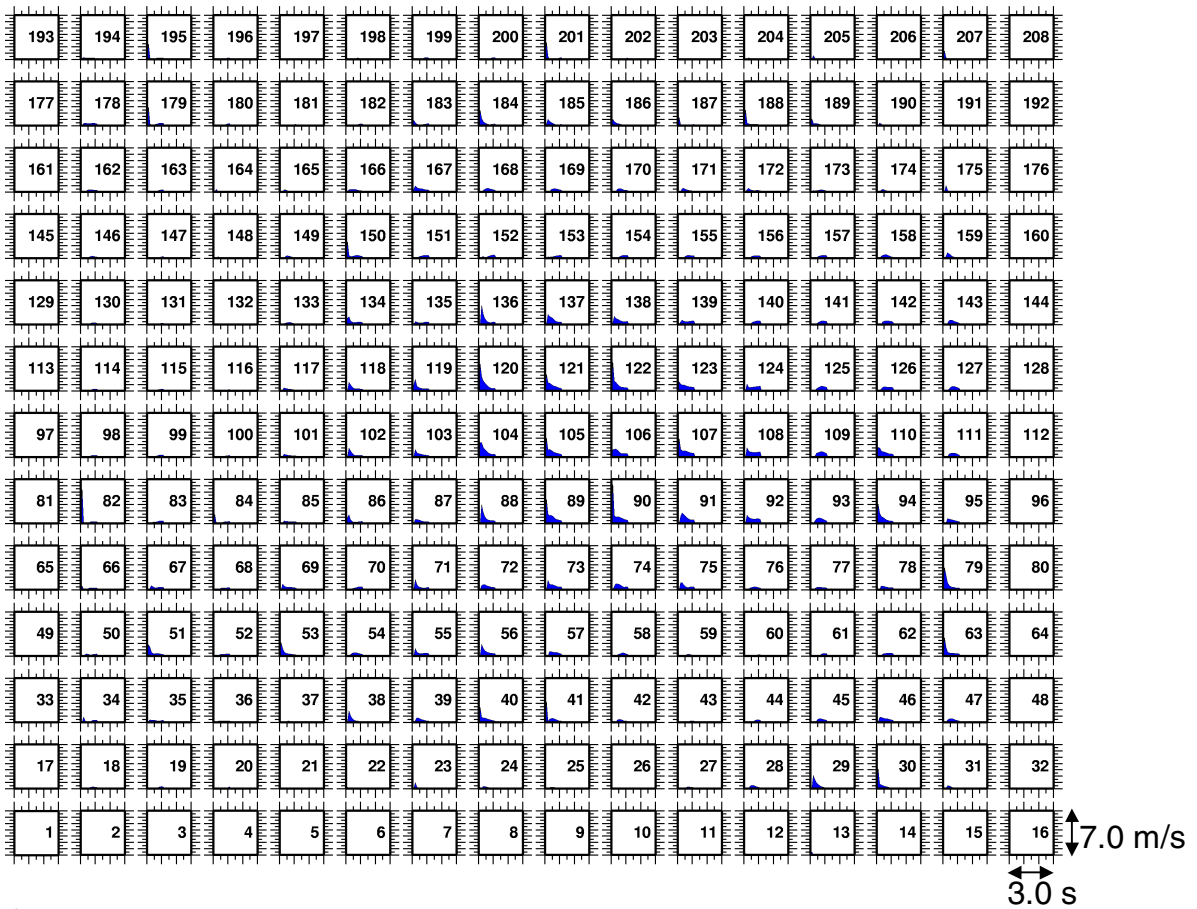


Figure 7. Slip velocity functions at the knots (vertices of subfaults) on the fault plane, extracted from the strong-motion inversion model.

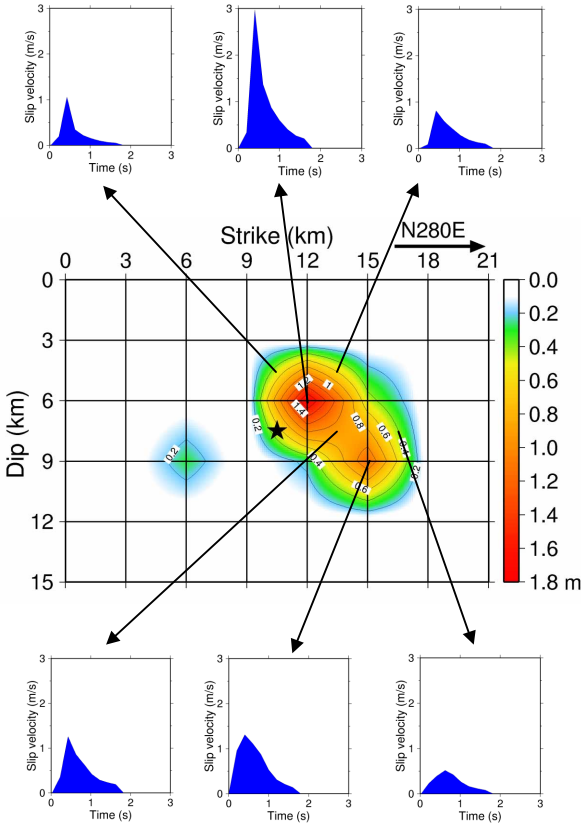


Figure 8. Extracted slip velocity functions at representative positions on the fault plane from the teleseismic source inversion result.

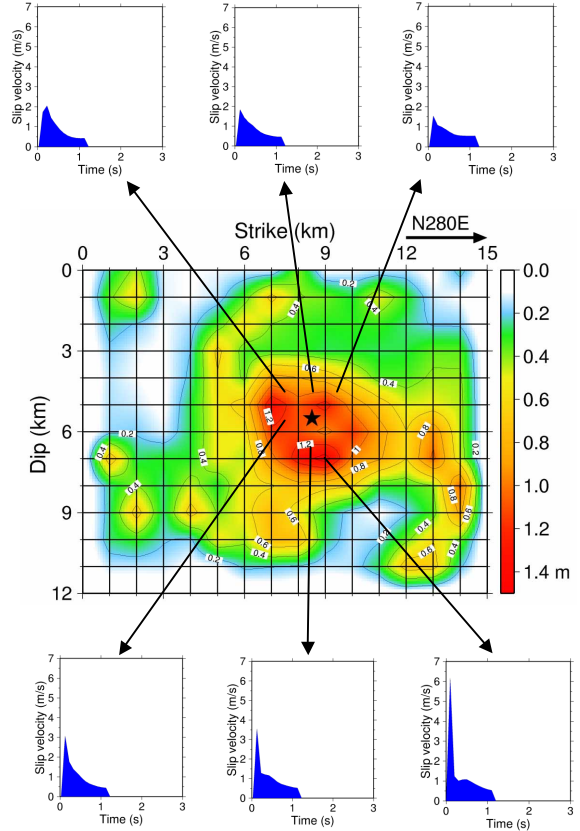


Figure 9. Extracted slip velocity functions at representative positions on the fault plane from the strong-motion inversion result.

In the present approach, since the derived slip velocity is continuous everywhere spatially and temporally, the fault rupture process can be seen in terms of slip velocity by the sequential snapshots. The snapshot at any time can be made from the slip velocity functions at the spatial knots shown in Figures 6 and 7. Figures 10 and 11 display sequential snapshots of the slip velocity in the time interval of 0.6 s, extracted from the teleseismic inversion and the strong-motion inversion results, respectively. They give clear and sharp images of the rupture and slip process. It may come from one of the advantages of the present approach that our representation of slip velocity has an explicit rupture propagation term so that the propagating rupture is involved in the slip velocity at any position over the fault plane.

CONCLUSIONS

We have developed a method for extracting slip velocity function continuous spatio-temporally over fault plane from existing conventional kinematic source inversion results. We also applied this method to the 26-March-1997 Northwestern Kagoshima earthquake from the teleseismic inversion and the strong-motion inversion models, respectively to demonstrate the feasibility of the method, and successfully extracted the slip velocity function from each inversion result. The slip velocity function extracted from the strong-motion inversion model has a higher resolution both in space and time compared to that from the teleseismic inversion model. The maximum peak velocity is 3 km/s for the teleseismic inversion case, while for the strong-motion inversion case it is 6 km/s. They are comparable to those for the 1995 Kobe earthquake estimated by previous studies (e.g. Matsushima and Kawase [1], Sekiguchi *et al.* [2])).

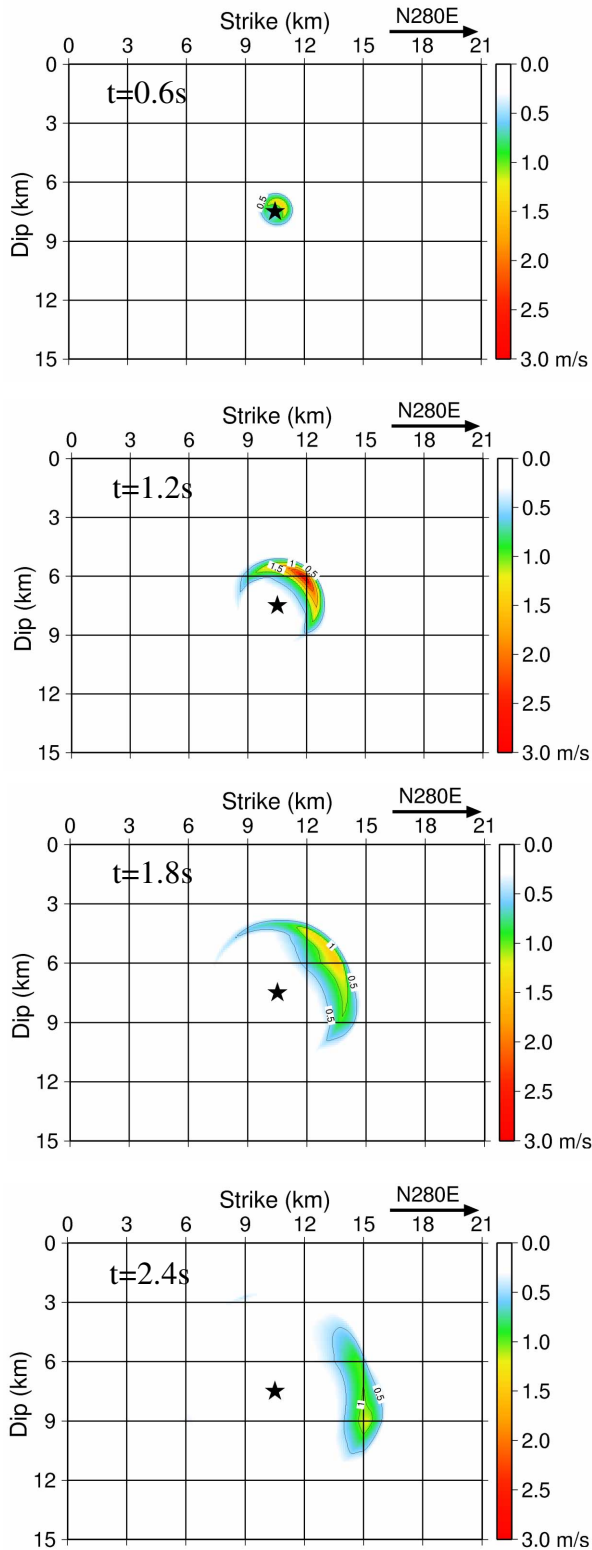


Figure 10. The history of rupture propagation in terms of slip velocity extracted from the teleseismic inversion result. The time interval is 0.6 s as labeled.

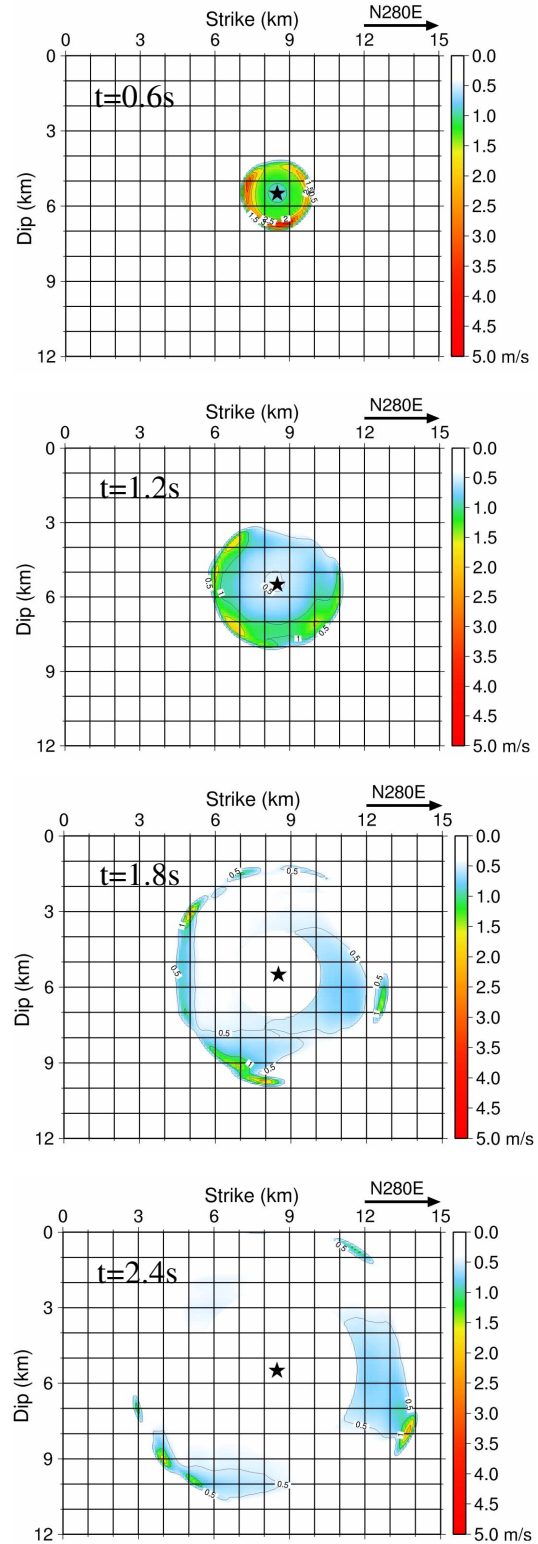


Figure 11. The history of rupture propagation in terms of slip velocity extracted from the strong-motion inversion result. The time interval is 0.6 s as labeled.

ACKNOWLEDGEMENTS

We used strong motion data provided by K-NET, National Research Institute for Earth Science and Disaster Prevention. This work was supported in part by the Special Coordinate Funds titled "Study on the master model for strong ground motion prediction toward earthquake disaster mitigation" from the Ministry of Education, Culture, Sports, Science and Technology of Japan.

REFERENCES

1. Matsushima S, Kawase H. "Multiple asperity source model of the Hyogo-ken Nanbu Earthquake of 1995 and strong motion simulation in Kobe." *J. Struct. Constr. Eng., AIJ*, 2000; (534): 33-40 (in Japanese with English abstract).
2. Sekiguchi H, K. Irikura K, Iwata T. "Source inversion for estimating the continuous slip distribution on a fault - introduction of Green's functions convolved with a correction function to give moving dislocation effects in subfaults." *Geophys. J. Int.*, 2002; 150(2): 377-391.
3. Olson, A. H., and R. J. Apsel: *Finite Faults and Inverse Theory with Applications to the 1979 Imperial Valley Earthquake*, Bulletin of Seismological Society of America, Vol. 72, No. 6, pp. 1969-2001.
4. Hartzell SH, Heaton TH. "Inversion of strong ground motion and teleseismic waveform data for the fault rupture history of the 1979 Imperial Valley, California, earthquake." *Bull. Seism. Soc. Am.* 1983; 73(6): 1553-1583.
5. Ide S, Takeo M. "Determination of constitutive relations of fault slip based on seismic wave analysis", *J. Geophys. Res.* 1997; 102(B12): 27379-27391.
6. Wu, C, Takeo, M, Ide, S. "Source Process of the Chi-Chi Earthquake: A joint Inversion of Strong Motion Data and Global Positioning System Data with a Multifault Model." *Bull. Seism. Soc. Am.* 2001; 91(5): 1128-1143.
7. Fujii Y, Nagano H, Takenaka H. "Source process of the 1997 Northwestern Kagoshima earthquakes inferred from teleseismic body waves." Abstracts in 2001 Japan Earth and Planetary Sci. Joint Meeting (CD-ROM) 2002: S051-010.
8. Miyakoshi K, Cho I, Petukhin A, Iwata T, Sekiguchi H. "Source characterization of inland crustal earthquakes in Japan using inverted high-resolution source models." this issue, Paper no. 849. 2004.
9. Kostrov, BV. "Selfsimilar problems of propagation of shear cracks." *PMM* 1964, 28(5): 889-898.